arXiv:hep-ex/0311028 v2 19 Dec 2003

DESY–03–182
November 2003

Isolated tau leptons in events with large missing transverse momentum at HERA

ZEUS Collaboration

Abstract

A search for events containing isolated tau leptons and large missing transverse momentum, not originating from the tau decay, has been performed with the ZEUS detector at the electron-proton collider HERA, using 130 pb^{-1} of integrated luminosity. A search was made for isolated tracks coming from hadronic tau decays. Observables based on the internal jet structure were exploited to discriminate between tau decays and quark- or gluon-induced jets. Three tau candidates were found, while $0.40^{+0.12}_{-0.13}$ were expected from Standard Model processes, such as charged current deep inelastic scattering and single $W^{\pm}$-boson production. To search for heavy-particle decays, a more restrictive selection was applied to isolate tau leptons produced together with a hadronic final state with high transverse momentum. Two candidate events survive, while 0.20 ± 0.05 events are expected from Standard Model processes.

The ZEUS Collaboration

S. Chekanov, M. Derrick, D. Krakauer, J.H. Loizides[1], S. Magill, S. Miglioranzi[1], B. Musgrave, J. Repond, R. Yoshida
Argonne National Laboratory, Argonne, Illinois 60439-4815, USA [n]

M.C.K. Mattingly
Andrews University, Berrien Springs, Michigan 49104-0380, USA

P. Antonioli, G. Bari, M. Basile, L. Bellagamba, D. Boscherini, A. Bruni, G. Bruni, G. Cara Romeo, L. Cifarelli, F. Cindolo, A. Contin, M. Corradi, S. De Pasquale, P. Giusti, G. Iacobucci, A. Margotti, A. Montanari, R. Nania, F. Palmonari, A. Pesci, G. Sartorelli, A. Zichichi
University and INFN Bologna, Bologna, Italy [e]

G. Aghuzumtsyan, D. Bartsch, I. Brock, S. Goers, H. Hartmann, E. Hilger, P. Irrgang, H.-P. Jakob, O. Kind, U. Meyer, E. Paul[2], J. Rautenberg, R. Renner, A. Stifutkin, J. Tandler, K.C. Voss, M. Wang, A. Weber[3]
Physikalisches Institut der Universität Bonn, Bonn, Germany [b]

D.S. Bailey[4], N.H. Brook, J.E. Cole, G.P. Heath, T. Namsoo, S. Robins, M. Wing
H.H. Wills Physics Laboratory, University of Bristol, Bristol, United Kingdom [m]

M. Capua, A. Mastroberardino, M. Schioppa, G. Susinno
Calabria University, Physics Department and INFN, Cosenza, Italy [e]

J.Y. Kim, Y.K. Kim, J.H. Lee, I.T. Lim, M.Y. Pac[5]
Chonnam National University, Kwangju, Korea [g]

A. Caldwell[6], M. Helbich, X. Liu, B. Mellado, Y. Ning, S. Paganis, Z. Ren, W.B. Schmidke, F. Sciulli
Nevis Laboratories, Columbia University, Irvington on Hudson, New York 10027 [o]

J. Chwastowski, A. Eskreys, J. Figiel, A. Galas, K. Olkiewicz, P. Stopa, L. Zawiejski
Institute of Nuclear Physics, Cracow, Poland [i]

L. Adamczyk, T. Bołd, I. Grabowska-Bołd[7], D. Kisielewska, A.M. Kowal, M. Kowal, T. Kowalski, M. Przybycień, L. Suszycki, D. Szuba, J. Szuba[8]
Faculty of Physics and Nuclear Techniques, AGH-University of Science and Technology, Cracow, Poland [p]

A. Kotański[9], W. Słomiński
Department of Physics, Jagellonian University, Cracow, Poland

V. Adler, U. Behrens, I. Bloch, K. Borras, V. Chiochia, D. Dannheim, G. Drews, J. Fourletova, U. Fricke, A. Geiser, P. Göttlicher[10], O. Gutsche, T. Haas, W. Hain, S. Hillert[11], B. Kahle, U. Kötz, H. Kowalski[12], G. Kramberger, H. Labes, D. Lelas, H. Lim, B. Löhr, R. Mankel, I.-A. Melzer-Pellmann, C.N. Nguyen, D. Notz, A.E. Nuncio-Quiroz, A. Polini, A. Raval, L. Rurua, U. Schneekloth, U. Stoesslein, G. Wolf, C. Youngman, W. Zeuner
Deutsches Elektronen-Synchrotron DESY, Hamburg, Germany

S. Schlenstedt
DESY Zeuthen, Zeuthen, Germany

G. Barbagli, E. Gallo, C. Genta, P. G. Pelfer
University and INFN, Florence, Italy [e]

A. Bamberger, A. Benen, N. Coppola
Fakultät für Physik der Universität Freiburg i.Br., Freiburg i.Br., Germany [b]

M. Bell, P.J. Bussey, A.T. Doyle, J. Ferrando, J. Hamilton, S. Hanlon, D.H. Saxon, I.O. Skillicorn
Department of Physics and Astronomy, University of Glasgow, Glasgow, United Kingdom [m]

I. Gialas
Department of Engineering in Management and Finance, Univ. of Aegean, Greece

B. Bodmann, T. Carli, U. Holm, K. Klimek, N. Krumnack, E. Lohrmann, M. Milite, H. Salehi, P. Schleper, S. Stonjek[11], K. Wick, A. Ziegler, Ar. Ziegler
Hamburg University, Institute of Exp. Physics, Hamburg, Germany [b]

C. Collins-Tooth, C. Foudas, R. Gonçalo[13], K.R. Long, A.D. Tapper
Imperial College London, High Energy Nuclear Physics Group, London, United Kingdom [m]

P. Cloth, D. Filges
Forschungszentrum Jülich, Institut für Kernphysik, Jülich, Germany

M. Kataoka[14], K. Nagano, K. Tokushuku[15], S. Yamada, Y. Yamazaki
Institute of Particle and Nuclear Studies, KEK, Tsukuba, Japan [f]

A.N. Barakbaev, E.G. Boos, N.S. Pokrovskiy, B.O. Zhautykov
Institute of Physics and Technology of Ministry of Education and Science of Kazakhstan, Almaty, Kazakhstan

D. Son
Kyungpook National University, Center for High Energy Physics, Daegu, South Korea [g]

K. Piotrzkowski
Institut de Physique Nucléaire, Université Catholique de Louvain, Louvain-la-Neuve, Belgium

F. Barreiro, C. Glasman[16], O. González, L. Labarga, J. del Peso, E. Tassi, J. Terrón, M. Vázquez, M. Zambrana
Departamento de Física Teórica, Universidad Autónoma de Madrid, Madrid, Spain [l]

M. Barbi, F. Corriveau, S. Gliga, J. Lainesse, S. Padhi, D.G. Stairs, R. Walsh
Department of Physics, McGill University, Montréal, Québec, Canada H3A 2T8 [a]

T. Tsurugai
Meiji Gakuin University, Faculty of General Education, Yokohama, Japan [f]

A. Antonov, P. Danilov, B.A. Dolgoshein, D. Gladkov, V. Sosnovtsev, S. Suchkov
Moscow Engineering Physics Institute, Moscow, Russia [j]

R.K. Dementiev, P.F. Ermolov, Yu.A. Golubkov[17], I.I. Katkov, L.A. Khein, I.A. Korzhavina, V.A. Kuzmin, B.B. Levchenko[18], O.Yu. Lukina, A.S. Proskuryakov, L.M. Shcheglova, N.N. Vlasov[19], S.A. Zotkin
Moscow State University, Institute of Nuclear Physics, Moscow, Russia [k]

N. Coppola, S. Grijpink, E. Koffeman, P. Kooijman, E. Maddox, A. Pellegrino, S. Schagen, H. Tiecke, J.J. Velthuis, L. Wiggers, E. de Wolf
NIKHEF and University of Amsterdam, Amsterdam, Netherlands [h]

N. Brümmer, B. Bylsma, L.S. Durkin, T.Y. Ling
Physics Department, Ohio State University, Columbus, Ohio 43210 [n]

A.M. Cooper-Sarkar, A. Cottrell, R.C.E. Devenish, B. Foster, G. Grzelak, C. Gwenlan[20], S. Patel, P.B. Straub, R. Walczak
Department of Physics, University of Oxford, Oxford United Kingdom [m]

A. Bertolin, R. Brugnera, R. Carlin, F. Dal Corso, S. Dusini, A. Garfagnini, S. Limentani, A. Longhin, A. Parenti, M. Posocco, L. Stanco, M. Turcato
Dipartimento di Fisica dell' Università and INFN, Padova, Italy [e]

E.A. Heaphy, F. Metlica, B.Y. Oh, J.J. Whitmore[21]
Department of Physics, Pennsylvania State University, University Park, Pennsylvania 16802 [o]

Y. Iga
Polytechnic University, Sagamihara, Japan [f]

G. D'Agostini, G. Marini, A. Nigro
Dipartimento di Fisica, Università 'La Sapienza' and INFN, Rome, Italy [e]

C. Cormack[22], J.C. Hart, N.A. McCubbin
Rutherford Appleton Laboratory, Chilton, Didcot, Oxon, United Kingdom [m]

C. Heusch
University of California, Santa Cruz, California 95064, USA [n]

I.H. Park
Department of Physics, Ewha Womans University, Seoul, Korea

N. Pavel
Fachbereich Physik der Universität-Gesamthochschule Siegen, Germany

H. Abramowicz, A. Gabareen, S. Kananov, A. Kreisel, A. Levy
Raymond and Beverly Sackler Faculty of Exact Sciences, School of Physics, Tel-Aviv University, Tel-Aviv, Israel [d]

M. Kuze
Department of Physics, Tokyo Institute of Technology, Tokyo, Japan [f]

T. Fusayasu, S. Kagawa, T. Kohno, T. Tawara, T. Yamashita
Department of Physics, University of Tokyo, Tokyo, Japan [f]

R. Hamatsu, T. Hirose[2], M. Inuzuka, H. Kaji, S. Kitamura[23], K. Matsuzawa
Tokyo Metropolitan University, Department of Physics, Tokyo, Japan [f]

M.I. Ferrero, V. Monaco, R. Sacchi, A. Solano
Università di Torino and INFN, Torino, Italy [e]

M. Arneodo, M. Ruspa
Università del Piemonte Orientale, Novara, and INFN, Torino, Italy [e]

T. Koop, G.M. Levman, J.F. Martin, A. Mirea
Department of Physics, University of Toronto, Toronto, Ontario, Canada M5S 1A7 [a]

J.M. Butterworth[24], R. Hall-Wilton, T.W. Jones, M.S. Lightwood, M.R. Sutton, C. Targett-Adams
Physics and Astronomy Department, University College London, London, United Kingdom [m]

J. Ciborowski[25], R. Ciesielski[26], P. Łużniak[27], R.J. Nowak, J.M. Pawlak, J. Sztuk[28], T. Tymieniecka[29], A. Ukleja[29], J. Ukleja[30], A.F. Żarnecki
Warsaw University, Institute of Experimental Physics, Warsaw, Poland [q]

M. Adamus, P. Plucinski
Institute for Nuclear Studies, Warsaw, Poland [q]

Y. Eisenberg, L.K. Gladilin[31], D. Hochman, U. Karshon M. Riveline
Department of Particle Physics, Weizmann Institute, Rehovot, Israel [c]

D. Kçira, S. Lammers, L. Li, D.D. Reeder, M. Rosin, A.A. Savin, W.H. Smith
Department of Physics, University of Wisconsin, Madison, Wisconsin 53706, USA [n]

A. Deshpande, S. Dhawan
Department of Physics, Yale University, New Haven, Connecticut 06520-8121, USA [n]

S. Bhadra, C.D. Catterall, S. Fourletov, G. Hartner, S. Menary, M. Soares, J. Standage
Department of Physics, York University, Ontario, Canada M3J 1P3 [a]

[1] also affiliated with University College London, London, UK
[2] retired
[3] self-employed
[4] PPARC Advanced fellow
[5] now at Dongshin University, Naju, Korea
[6] now at Max-Planck-Institut für Physik, München,Germany
[7] partly supported by Polish Ministry of Scientific Research and Information Technology, grant no. 2P03B 122 25
[8] partly supp. by the Israel Sci. Found. and Min. of Sci., and Polish Min. of Scient. Res. and Inform. Techn., grant no.2P03B12625
[9] supported by the Polish State Committee for Scientific Research, grant no. 2 P03B 09322
[10] now at DESY group FEB
[11] now at Univ. of Oxford, Oxford/UK
[12] on leave of absence at Columbia Univ., Nevis Labs., N.Y., US A
[13] now at Royal Holoway University of London, London, UK
[14] also at Nara Women's University, Nara, Japan
[15] also at University of Tokyo, Tokyo, Japan
[16] Ramón y Cajal Fellow
[17] now at HERA-B
[18] partly supported by the Russian Foundation for Basic Research, grant 02-02-81023
[19] now at University of Freiburg, Germany
[20] PPARC Postdoctoral Research Fellow
[21] on leave of absence at The National Science Foundation, Arlington, VA, USA
[22] now at Univ. of London, Queen Mary College, London, UK
[23] present address: Tokyo Metropolitan University of Health Sciences, Tokyo 116-8551, Japan
[24] also at University of Hamburg, Alexander von Humboldt Fellow
[25] also at Łódź University, Poland
[26] supported by the Polish State Committee for Scientific Research, grant no. 2 P03B 07222
[27] Łódź University, Poland
[28] Łódź University, Poland, supported by the KBN grant 2P03B12925
[29] supported by German Federal Ministry for Education and Research (BMBF), POL 01/043
[30] supported by the KBN grant 2P03B12725
[31] on leave from MSU, partly supported by University of Wisconsin via the U.S.-Israel BSF

[a] supported by the Natural Sciences and Engineering Research Council of Canada (NSERC)

[b] supported by the German Federal Ministry for Education and Research (BMBF), under contract numbers HZ1GUA 2, HZ1GUB 0, HZ1PDA 5, HZ1VFA 5

[c] supported by the MINERVA Gesellschaft für Forschung GmbH, the Israel Science Foundation, the U.S.-Israel Binational Science Foundation and the Benozyio Center for High Energy Physics

[d] supported by the German-Israeli Foundation and the Israel Science Foundation

[e] supported by the Italian National Institute for Nuclear Physics (INFN)

[f] supported by the Japanese Ministry of Education, Culture, Sports, Science and Technology (MEXT) and its grants for Scientific Research

[g] supported by the Korean Ministry of Education and Korea Science and Engineering Foundation

[h] supported by the Netherlands Foundation for Research on Matter (FOM)

[i] supported by the Polish State Committee for Scientific Research, grant no. 620/E-77/SPB/DESY/P-03/DZ 117/2003-2005

[j] partially supported by the German Federal Ministry for Education and Research (BMBF)

[k] partly supported by the Russian Ministry of Industry, Science and Technology through its grant for Scientific Research on High Energy Physics

[l] supported by the Spanish Ministry of Education and Science through funds provided by CICYT

[m] supported by the Particle Physics and Astronomy Research Council, UK

[n] supported by the US Department of Energy

[o] supported by the US National Science Foundation

[p] supported by the Polish State Committee for Scientific Research, grant no. 112/E-356/SPUB/DESY/P-03/DZ 116/2003-2005,2 P03B 13922

[q] supported by the Polish State Committee for Scientific Research, grant no. 115/E-343/SPUB-M/DESY/P-03/DZ 121/2001-2002, 2 P03B 07022

1 Introduction

Events with isolated leptons and large missing transverse momentum in $e^{\pm}p$-collisions at HERA can be a signature for processes beyond the Standard Model (SM). The H1 and ZEUS Collaborations have previously reported searches for such events in the cases where the lepton is an electron[1] or a muon [1, 2, 3, 4]. This paper presents a search for events with an isolated tau lepton and missing transverse momentum which does not originate from the tau decay ($ep \to \tau\chi X$, where χ denotes one or more particles not interacting inside the detector). Such events are expected to occur at low rates in the SM from decays of $W^{\pm}$ bosons into $\tau^{\pm}\overset{(-)}{\nu}_{\tau}$, where the $W^{\pm}$ is produced radiatively from the quark or the beam lepton. Events with a large hadronic transverse momentum in addition to an isolated lepton are of particular interest since the SM background falls steeply with increasing hadronic transverse momentum. Such events may result from the decay of a heavy particle. One possible source for this signature would be the production of single top quarks through flavour changing neutral currents (FCNC), with subsequent decay $t \to bW^{+}$, as predicted by many theories beyond the SM [5]. Production of stop quarks in R-parity (R_p) violating SUSY models [6] with subsequent two-body decay (e.g. $\tilde{t} \to \tau b$) or R_p-conserving three-body decay modes ($\tilde{t} \to \tau\tilde{\nu_{\tau}}b$, $\tilde{\tau}\nu_{\tau}b$) are also potential sources.

The tau leptons were identified from their hadronic decay by requiring a collimated and low-multiplicity hadronic jet. Charged current (CC) and neutral current (NC) interactions, with gluon- and quark-induced jets, are large potential backgrounds to this process. Restrictive conditions applied to jets reduced such backgrounds to a rate comparable to that of single $W^{\pm}$ production.

This paper is organized as follows. Section 2 describes the ZEUS detector and the experimental conditions. Section 3 introduces the $e^{\pm}p$-interaction processes that were considered in this analysis, and their Monte Carlo simulation. The identification of tau leptons, which is based on an independent study, is introduced in Section 4. Section 5 presents the selection requirements for events with isolated tau leptons. The results of the analysis are discussed in Section 6. Section 7 gives the conclusions.

2 Experimental conditions

The data used in this analysis were collected with the ZEUS detector at HERA and correspond to an integrated luminosity of 47.9 ± 0.9 (65.5 ± 1.5) pb^{-1} for $e^{+}p$ collisions taken

[1] Here and in the following, the term 'electron' denotes generically both the electron (e^{-}) and the positron (e^{+}).

during 1994-1997 (1999-2000) and $16.7 \pm 0.3\,\mathrm{pb}^{-1}$ for $e^- p$ collisions taken during 1998-99. During 1994-97 (1998-2000), HERA operated with protons of energy $E_p = 820$ GeV (920 GeV) and electrons of energy $E_e = 27.5$ GeV, yielding a centre-of-mass energy of $\sqrt{s} = 300$ GeV (318 GeV).

The ZEUS detector is described in detail elsewhere [7,8]. The main components used in this analysis were the central tracking detector (CTD) [9], positioned in a 1.43 T solenoidal magnetic field, and the uranium-scintillator sampling calorimeter (CAL) [10].

Tracking information is provided by the CTD, in which the momenta of tracks in the polar-angle[2] region $15^\circ < \theta < 164^\circ$ are reconstructed. The CTD consists of 72 cylindrical drift chamber layers, organised in nine superlayers. The relative transverse-momentum resolution for full-length tracks can be parameterised as $\sigma(p_T)/p_T = 0.0058\ p_T \oplus 0.0065 \oplus 0.0014/p_T$, with p_T in GeV.

The CAL covers 99.7% of the total solid angle. It is divided into three parts with a corresponding division in θ, as viewed from the nominal interaction point: forward (FCAL, $2.6^\circ < \theta < 36.7^\circ$), barrel (BCAL, $36.7^\circ < \theta < 129.1^\circ$), and rear (RCAL, $129.1^\circ < \theta < 176.2^\circ$). Each of the CAL parts is subdivided into towers which in turn are segmented longitudinally into one electromagnetic (EMC) and one (RCAL) or two (FCAL, BCAL) hadronic (HAC) sections. The smallest subdivision of the CAL is called a cell. Under test-beam conditions, the CAL single-particle relative energy resolution is $\sigma(E)/E = 0.18/\sqrt{E}$ for electrons and $\sigma(E)/E = 0.35/\sqrt{E}$ for hadrons, with E in GeV. In addition, the readout of the individual CAL cells provides timing information, with a resolution better than 1 ns for energy depositions larger than 4.5 GeV.

The luminosity was measured using the Bethe-Heitler reaction $e^\pm p \to e^\pm \gamma p$. The resulting small-angle energetic photons were measured by the luminosity monitor [11], a lead-scintillator calorimeter placed in the HERA tunnel at $Z = -107$ m. A three-level trigger was used to select events online [7,12].

3 Monte Carlo simulation

In the following, processes which may lead to the event topology of interest, and their Monte Carlo (MC) simulations, are described. All generated MC events were passed through the GEANT 3.13-based [13] ZEUS detector- and trigger-simulation programs [7]. They were reconstructed and analysed by the same program chain as the data.

[2] The ZEUS coordinate system is a right-handed Cartesian system, with the Z axis pointing in the proton beam direction, referred to as the "forward direction", and the X axis pointing left towards the centre of HERA. The coordinate origin is at the nominal interaction point.

$W^{\pm}$ production: $e^{\pm}p \to e^{\pm}WX$. The production of real $W^{\pm}$ bosons with subsequent decay $W^{\pm} \to \tau^{\pm}\overset{(-)}{\nu}_{\tau}$ is the only SM process with sizeable cross section leading to events with an isolated tau lepton and missing transverse momentum. Single $W^{\pm}$ production was simulated using the event generator EPVEC [14]. The hadronisation of the partonic final state and the decays of the tau leptons were performed by JETSET [15]. As a cross check, control MC samples were used with the tau decays performed by TAUOLA 2.6 [16]. Recent cross-section calculations including $\mathcal{O}(\alpha^2\alpha_s)$ QCD corrections [17] and using the CTEQ4M [18] (ACFGP [19]) proton (photon) parton density functions were used to reweight the EPVEC samples. The total cross section for $W^{\pm}$ production is 1.0 pb (1.2 pb) for an $e^{\pm}p$ centre-of-mass energy of $\sqrt{s} = 300\,\text{GeV}$ (318 GeV). The contribution of the CC process $e^{\pm}p \to \overset{(-)}{\nu}_{e}W^{\pm}X$ is about 5% of that from the neutral current process and was neglected [3].

Charged current deep inelastic scattering (CC DIS): $e^{\pm}p \to \overset{(-)}{\nu}_{e}X$. Events from CC DIS interactions can mimic the selected topology if a particle from the hadronic final state is misidentified as an isolated tau lepton. The CC DIS events were simulated using the event generator DJANGO6 [20], an interface to the MC programs HERACLES 4.5 [21] and LEPTO 6.5 [22]. Leading-order QCD and electroweak radiative corrections were included and higher-order QCD effects were simulated via parton cascades using the colour-dipole model (CDM) as implemented in ARIADNE [23] or matrix elements and parton showers (MEPS) based on a leading-logarithmic approximation as implemented in LEPTO. The hadronisation of the partonic final state was performed by JETSET. The CTEQ4D [18] parameterisations for the parton density functions (PDFs) in the proton were used.

Neutral current deep inelastic scattering (NC DIS): $e^{\pm}p \to e^{\pm}X$. The scattered electron or a jet from the hadronic system in an NC DIS event can be misidentified as an isolated tau lepton. This can lead to the selected event topology, if combined with apparent missing transverse momentum, which may arise from leptonic decays of charm or bottom quarks, fluctuations in the detector response or undetected particles due to the limited geometric acceptance of the detector. The NC DIS events were simulated in the same framework as the CC DIS events. The CTEQ5D [24] parameterisations for the proton PDFs were used.

Photoproduction of jets: $\gamma p \to X$. Background from hard scattering photoproduction processes can contribute to the selected event topology if a particle from the hadronic final state is misidentified as a tau lepton and apparent missing transverse momentum is present, arising from the sources described above. Resolved and direct photoproduction processes were simulated using PYTHIA 5.7 [25].

Lepton-pair production: $e^{\pm}p \to e^{\pm}l^{\pm}l^{\mp}X$, $l = e, \mu, \tau$. Pair production of leptons via the Bethe-Heitler process can lead to events with the selected topology, if one of the leptons escapes detection or is misidentified as a QCD jet and a mismeasurement causes missing transverse momentum. Lepton-pair production was simulated using the GRAPE dilepton

generator [26], including both the elastic and inelastic components at the proton vertex.

Single-top production in theories beyond the SM: $e^{\pm}q \to e^{\pm}t \to e^{\pm}bW^{+}$. A significant number of single top quarks with subsequent decays into a b quark and a W^{+} boson could be produced if the top quarks were to be produced via anomalous effective couplings, including FCNC of the type tuV (u = up-type quark in the proton, $V = \gamma, Z^{0}$) [5]. An isolated tau lepton and a neutrino from the W^{+} decay lead to the selected event topology. The large mass of the top quark could result in large transverse momenta of its decay products, which through the subsequent b-quark decay would produce a large hadronic transverse momentum in the detector. In the current paper, the anomalous production of single top quarks was used as a template for processes involving the production of heavy particles with tau leptons in the decay chain. Single-top production through FCNC processes in $e^{\pm}p$ collisions was simulated using the HEXF generator [27].

4 Tau identification

The search for tau leptons is based on their hadronic decays. The narrow, "pencil-like", shape and the low charged-particle multiplicity of the tau jets were used to distinguish them from quark- and gluon-induced jets [28].

4.1 Jet observables

The longitudinally invariant k_T cluster algorithm [29] was used in the inclusive mode [30] to reconstruct jets from the energy deposits in the CAL cells. The jet search was performed in the $\eta - \phi$ plane of the laboratory frame, where η_i and ϕ_i, the pseudorapidity and azimuthal angle of each CAL cell, were calculated using the primary event vertex as reconstructed in the CTD. The axis of each jet was defined according to the Snowmass convention [31], where $\eta_{\rm jet}$ ($\phi_{\rm jet}$) was the transverse-energy-weighted mean pseudorapidity (azimuth angle) of all the cells belonging to the jet. The jet transverse energy, $E_T^{\rm jet}$, was reconstructed as the sum of the transverse energies of the cells belonging to the jet and was corrected for detector effects such as energy losses in the inactive material in front of the CAL [32].

The internal jet structure is generally well described by the MC simulations [33,34]. For this analysis, it was characterised by six observables:

- the first moment of the radial extension of the jet

$$R_{\rm mean} = \langle R \rangle = \frac{\sum_i E_i \cdot R_i}{\sum_i E_i},$$

where the sum runs over the CAL cells associated to the jet, E_i is the energy of the cell i and R_i is defined as $R_i = \sqrt{\Delta\phi_i^2 + \Delta\eta_i^2}$, where $\Delta\phi_i$ ($\Delta\eta_i$) is the difference between the azimuthal angle (pseudorapidity) of the calorimeter cell i and the jet axis;

- the second moment of the radial extension of the jet

$$R_{\rm rms} = \sqrt{\frac{\sum_i E_i(\langle R\rangle - R_i)^2}{\sum_i E_i}};$$

- the first moment of the projection of the jet onto its axis

$$L_{\rm mean} = \langle L\rangle = \frac{\sum_i E_i \cdot \cos\alpha_i}{\sum_i E_i},$$

where α_i is the angle between the cell i and the jet axis;

- the second moment of the projection of the jet onto its axis

$$L_{\rm rms} = \sqrt{\frac{\sum_i E_i(\langle L\rangle - \cos\alpha_i)^2}{\sum_i E_i}};$$

- the number of subjets ($N_{\rm subj}$) with a $y_{\rm cut}$ of $5 \cdot 10^{-4}$.
The subjet multiplicity identifies the number of localised energy depositions within a jet that can be resolved using a resolution-criterion $y_{\rm cut}$. The number of subjets was found by applying the same algorithm as was initially used to find jets. An exact definition can be found elsewhere [35,36,34];

- the invariant mass, $M_{\rm jet}$, of the jet four-vector, calculated from the cells associated to the jet. The particles of the jet were assumed to be massless.

4.2 Control selection

The tau-identification procedure was determined using event samples selected independently from those used for the analysis. Monte Carlo events from single $W^{\pm}$ production, where the $W^{\pm}$ decays to a tau lepton and a neutrino and the tau lepton decays hadronically ($W^{\pm} \to \tau^{\pm}\overset{(-)}{\nu}_{\tau}, \tau \to hadrons$), were used as signal. The background simulation was based on an inclusive sample of MC CC DIS events.

An inclusive CC DIS data sample was used to monitor the quality of the simulation [37]. To obtain this sample, large missing transverse momentum and the existence of at least one jet with $E_T^{\rm jet} > 5\,{\rm GeV}$ in the polar-angle range $15^\circ < \theta_{\rm jet} < 164^\circ$ were required. Electrons from badly reconstructed NC DIS events with large apparent missing transverse momentum were suppressed by rejecting jets that were back-to-back with the hadronic

system. Remaining electrons were rejected based on the fraction of electromagnetic energy and on the fraction of the jet energy carried by the leading track pointing in the direction of the jet [38].

Figure 1 shows the comparison of the inclusive CC DIS data sample and the MC CC events in each of the six jet-shape observables. For each event, only the jet with the largest value of the tau discriminant, as defined below, enters. The agreement between the data and the simulation is good. The expected signal from tau decay is also shown. A difference in the shapes between the tau jets and the quark- or gluon-induced jets is evident for all six variables.

4.3 Tau discriminant

To separate the signal from the background, the six jet-shape observables were combined in a discriminant $\mathcal{D}$, given for any point, $\vec{x}$, in the phase space, where

$$\vec{x} = (-\log(\mathrm{R_{mean}}), -\log(\mathrm{R_{rms}}), -\log(1-\mathrm{L_{mean}}), -\log(\mathrm{L_{rms}}), \mathrm{N_{subj}}, \mathrm{M_{jet}}),$$

as:

$$\mathcal{D}(\vec{x}) = \frac{\rho_{\mathrm{sig}}(\vec{x})}{\rho_{\mathrm{sig}}(\vec{x}) + \rho_{\mathrm{bg}}(\vec{x})},$$

where ρ_{sig} and ρ_{bg} are the density functions of the signal and the background events, respectively. The signal and background densities, sampled using MC simulations, were calculated using a probability-density-estimation method based on range searching (PDE-RS) [39]. For any given jet with phase-space coordinates $\vec{x}$, the signal and background densities were evaluated from the number of corresponding signal and background jets in a six-dimensional box of fixed size centred around $\vec{x}$. Figure 2 shows the distribution of $\mathcal{D}$ for the MC-generated signal and background events and for the data selection. For each event, the jet with the largest value of the discriminant enters. The data are well described by the MC simulation for the inclusive CC selection. The tau signal tends to have large discriminant values ($\mathcal{D} \to 1$) and is clearly separated from the CC DIS background at low discriminant values ($\mathcal{D} \to 0$).

The quality of the tau selection is characterised by the efficiency of the signal selection ϵ_{sig}, the rejection of the background, R, and the separation power, S, which are defined for a given cut on the discriminant, $\mathcal{D}_{\mathrm{cut}}$, as follows:

$$\begin{aligned} \epsilon_{\mathrm{sig}} &= N_{\mathrm{sig,selected}}/N_{\mathrm{sig,total}} \\ R &= N_{\mathrm{bg,total}}/N_{\mathrm{bg,selected}} \\ S &= \sqrt{R} \cdot \epsilon_{\mathrm{sig}}. \end{aligned}$$

In the equations above, $N_{\mathrm{sig,total}}$ and $N_{\mathrm{bg,total}}$ are the total number of signal and background events, respectively, and $N_{\mathrm{sig,selected}}$ and $N_{\mathrm{bg,selected}}$ are the number of signal and background events after applying a cut of $\mathcal{D} > \mathcal{D}_{\mathrm{cut}}$, respectively. The cut on $\mathcal{D}$ was optimised for maximal separation power. The optimisation resulted in a value of $\mathcal{D} > 0.95$, for which a signal efficiency $\epsilon_{\mathrm{sig}} = 31 \pm 0.2\%$, a background rejection $R = 179 \pm 6$ and a separation power $S = 4.1 \pm 0.1$ were obtained. The quoted uncertainties are the statistical uncertainties due to the limited number of generated MC events. When restricting the selection to jets with only one track, as is relevant for the search for one-prong hadronic tau decays, the optimisation again resulted in a value of $\mathcal{D} > 0.95$. In this case the signal efficiency was $\epsilon_{\mathrm{sig}} = 22 \pm 0.2\%$, the background rejection was $R = 637 \pm 41$ and the separation was $S = 5.5 \pm 0.2$. These results are independent of the model chosen for the simulation of the QCD cascade in the CC DIS simulation (CDM or MEPS).

4.4 Misidentification of QCD jets and electrons

Both the suppression of QCD jets and the probability to misidentify electrons as tau jets were determined from samples of simulated NC DIS events and a selection of NC DIS data events [40], where an electron is scattered back-to-back to a jet in the detector. The main selection criteria were $Q^2 > 400\,\mathrm{GeV}^2$, where Q^2 is the virtuality of the exchanged boson, a well reconstructed electron and at least one jet in the acceptance of the detector.

To determine the rejection factor for QCD jets, the electron-rejection cuts from the CC DIS control selection described above were first applied to all jets in the samples. For the surviving one-track jets, the tau discriminant gives a further rejection factor of $R = 550$. This result is in agreement with the results from the CC DIS MC. No significant dependence of the rejection on the transverse energy of the jets was found. The results on the jet misidentification are the same in the data and in the simulation.

To determine the electron rejection, events in the NC DIS MC which had no well-identified electron were also considered. The upper limit on the fraction of NC DIS electrons that passed the tau selection and the CC DIS control-selection cuts was 3×10^{-6}. No difference between data and simulation was observed.

5 Event selection

The event selection closely follows the previous ZEUS search [4] for events with isolated leptons and large missing transverse momentum. The selection is based on the requirement of an isolated tau lepton, decaying to one charged particle, together with large missing transverse momentum. In a final selection stage, events with large values of

the hadronic transverse momentum were isolated. Details of the analysis can be found elsewhere [37]. In the following, only the main selection criteria are described.

5.1 Preselection of isolated tau events

A preselection of tau-candidate events was made as follows:

- cuts on the CAL timing and Z coordinate ($|Z| < 50$ cm) of the event vertex along with algorithms based on the pattern of tracks in the CTD were used to reject events not originating from $e^{\pm}p$ collisions;
- a large missing transverse momentum was required, $p_T^{\rm CAL} > 20\,{\rm GeV}$, where $p_T^{\rm CAL}$ was reconstructed using the energy deposited in the CAL cells, after corrections for non-uniformity and dead material located in front of the CAL [41];
- the selected events had to contain at least one jet, reconstructed as described in Section 4.1, with a transverse energy $E_T^{\rm jet} > 5\,{\rm GeV}$ within the range of $-1.0 < \eta < 2.5$;
- a track with transverse momentum $p_T^{\rm track} > 5\,{\rm GeV}$, associated with the event vertex and pointing in the direction of a tau-candidate jet, was required. It had to pass through at least three radial superlayers of the CTD (corresponding to $\theta \gtrsim 0.3\,{\rm rad}$) and to have $\theta < 2\,{\rm rad}$. The track was required to be isolated with respect to all other tracks and jets in the event: $D_{\rm trk} > 0.5$ and $D_{\rm jet} > 1.8$, where $D_{\rm trk}$ and $D_{\rm jet}$ are the separation of the given track in the $\{\eta, \phi\}$-plane from the nearest neighbouring track and the nearest neighbouring jet in the event, respectively;
- isolated tracks that were identified as electrons or muons[3] were rejected. An additional electron rejection was applied based on the fraction of electromagnetic jet energy and on the fraction of jet energy carried by the isolated track. Remaining electron-type events with a topology characteristic for NC DIS events were rejected by requiring the acoplanarity, $\phi_{\rm acopl}^{\rm trk}$, to be greater than 8°, where $\phi_{\rm acopl}^{\rm trk}$ is defined as the azimuthal angle between the isolated track and the vector which balances the hadronic system. The four-vector of the hadronic system was calculated by subtracting the four-vector of the tau-candidate jet from the four-vector obtained from the energy deposited in the CAL cells.

After this preselection, seven events remained, while $2.2^{+0.39}_{-0.58}$ are expected from SM background (18% of the SM background came from single $W^{\pm}$ boson production). Table 1 summarises the event yields at different selection stages. The quoted uncertainties on the SM expectations are discussed in Section 5.3. The discriminant distribution for these

[3] Electron candidates were identified using an algorithm that combined CAL and CTD information [42]. The identification of muons was based on the pattern of energy deposits in the CAL [37].

seven events is shown in Fig. 3a as $-\log(1-\mathcal{D})$, to emphasise the high-discriminant region.

Three out of the seven events have a tau discriminant $\mathcal{D} > 0.95$ and are therefore likely to come from tau decay. After applying the cut $\mathcal{D} > 0.95$, $0.40^{+0.12}_{-0.13}$ events are expected from SM background (43% from single $W^{\pm}$-boson production). Figure 3b shows the distribution of the transverse momentum of the hadronic system, $p_T^{\rm had}$, after applying the cut at $\mathcal{D} > 0.95$.

The online event selection required significant missing transverse momentum and a reconstructed vertex consistent with an $e^{\pm}p$ interaction. The efficiency of this online selection for the kinematic range of interest was found to be 100% for simulated events.

5.2 Selection of events with high hadronic transverse momentum

To design the final cut for events with high $p_T^{\rm had}$, the single-top MC was used as a template for the production and decay of a heavy state. Following the published analysis in the electron and muon channels, an optimisation was performed, resulting in a cut at $p_T^{\rm had} > 25\,\text{GeV}$, which gave the best separation between the single-top events and the SM background. Two events remained in the data, while 0.20 ± 0.05 events are expected from the SM (49% from single $W^{\pm}$-boson production). With a higher cut at $p_T^{\rm had} > 40\,\text{GeV}$, one event remains in the data, while 0.07 ± 0.02 events are expected from the SM (71% from single $W^{\pm}$-boson production). Figure 4 shows event displays of the two events with large values of $p_T^{\rm had}$. Selected event variables for the two candidates are given in Table 2. Both events were found at large acoplanarity. The transverse mass was calculated from the tau-candidate jet and the missing transverse momentum as $M_T = \sqrt{2 p_T^{\rm jet} p_T^{\rm CAL}(1-\cos(\delta\phi_{\rm jet}))}$, where $\delta\phi_{\rm jet}$ is the angular difference in the azimuthal plane between the tau jet and the direction of $p_T^{\rm CAL}$. Both events were identified in the $e^{+}p$ data sample.

5.3 Systematic uncertainties

The errors on the background-expectation values were obtained as the quadratic sum of the statistical uncertainties of the generated MC events and each of the following systematic uncertainties:

- *Simulation of the QCD cascade.* The use of MEPS instead of CDM to estimate both the NC DIS and CC DIS background gave a change of up to -20% in the total background estimation;

- *Track selection.* A variation of the track-quality requirements and the angular range of the track selection resulted in changes of up to $\pm 15\%$ in the background estimation;
- *W cross section.* The uncertainty for the expectation from single $W^{\pm}$-boson production, after including higher-order QCD corrections by reweighting the LO MC samples [17], was estimated to be 15%;
- *Tau-decay simulation.* As a cross check, TAUOLA was used instead of JETSET for the simulation of the tau decays originating from single $W^{\pm}$-boson production. The TAUOLA program takes into account polarisation effects, whereas in JETSET the tau leptons are always decayed isotropically in their rest frame. The influence of the tau-decay treatment on the jet-shape observables and on the efficiency for the event selection was found to be negligible;
- *Tau-discriminant method.* Both the CC DIS control selection and the tau-search analysis were repeated with modified sets of jet-shape observables. In addition, the box size used to evaluate the signal and background densities was varied. The dependence on these parameters was negligible;
- *Calorimeter energy scale.* The uncertainty of $\pm 1\%$ on the absolute energy scale of both the electromagnetic and the hadronic parts of the CAL resulted in changes of up to $\pm 4\%$ in the SM background estimation.

6 Discussion of results

Table 3 gives the result for the final selection in the tau channel as well as the results of the previous search in the electron and muon channel [4] for two different values of the cut on p_T^{had}. In the electron (muon) channel, two (five) events were observed for $p_T^{\mathrm{had}} > 25\,\mathrm{GeV}$, in good agreement with the SM prediction. No event was observed in either channel for $p_T^{\mathrm{had}} > 40\,\mathrm{GeV}$. In combination with a search in the hadronic decay channel of the $W^{\pm}$ boson, where no excess above the SM prediction was found, a limit on the cross section for single-top production of $\sigma(ep \to etX, \sqrt{s} = 318\,\mathrm{GeV}) < 0.225\,\mathrm{pb}$ at 95% C.L. was obtained [4]. For the tau channel, two events were observed for $p_T^{\mathrm{had}} > 25\,\mathrm{GeV}$. Only hadronic tau decays were considered and very restrictive selection cuts had to be applied to suppress the large background from electrons and quark- or gluon-induced jets. Therefore the selection efficiency for SM $W^{\pm}$ production is much smaller in the tau channel than in the electron and muon channels.

The Poisson probability to observe two or more events when 0.20 ± 0.05 events are expected is 1.8%, where the uncertainty on the SM prediction was taken into account. The observed events would correspond to a cross section for single-top production that is much higher than the excluded cross section, if the SM branching ratios for the top quark are assumed.

In addition, single-top production produces positively charged leptons, and single anti-top production from protons is relatively suppressed by the parton densities. Therefore the observed events are unlikely to be explained by the hypothesis of single-top production.

R_p-violating SUSY models can explain enhanced tau-production rates above the SM expectations. Moreover, if third-generation sleptons are lighter than sleptons of the first and second generation, a corresponding enhancement for electrons and muons could be strongly suppressed. In such models, the stop quark can be directly produced at HERA via an R_p-violating Yukawa coupling and subsequently decay through R_p-violating or gauge couplings. In particular, the three-body gauge decay $\tilde{t} \to \tau\tilde{\nu_\tau}b$, $\tilde{\tau}\nu_\tau b$ with the subsequent decays $\tilde{\tau} \to \tau\tilde{\chi}^0$, $\tilde{\nu_\tau} \to \nu_\tau\tilde{\chi}^0$ would produce a final state with the characteristics of the observed events: a high-p_T tau lepton at large acoplanarity angle, missing transverse momentum and large hadronic transverse momentum. However, in this case the tau candidate has the same charge as the incoming lepton beam, which is only the case for one of the two events surviving the cuts.

7 Conclusion

A search for events containing isolated tau leptons, large missing transverse momentum and large hadronic transverse momentum, produced in $e^{\pm}p$ collisions at HERA, has been performed using 130 pb^{-1} of integrated luminosity. Such a signature could be produced within the framework of many theories beyond the Standard Model. The selection required isolated tracks with associated pencil-like jets coming from hadronic tau decays. A multi-observable discrimination technique was used, exploiting the internal jet structure to discriminate between hadronic tau decays and quark- or gluon-induced jets. Three isolated tau candidates were found, while $0.40^{+0.12}_{-0.13}$ were expected from Standard Model processes, mainly from charged current deep inelastic scattering and single $W^{\pm}$-boson production. A more restrictive selection was applied to isolate tau leptons in events with large missing transverse momentum produced together with a hadronic final state with high transverse momentum, as expected from the decay of a heavy particle. Two candidate events with a transverse momentum of the hadronic system $p_T^{\mathrm{had}} > 25\,\mathrm{GeV}$ have been observed, while 0.20 ± 0.05 events were expected from Standard Model processes. The Poisson probability to observe two or more events, assuming only SM contribution, is 1.8%, so a statistical fluctuation cannot be excluded. When considered together with previously published results in the electron and muon channels, the two candidates are unlikely to originate from anomalous single-top production or any other process where the tau lepton is produced through the decay of a $W^{\pm}$ boson.

Acknowledgements

We thank the DESY Directorate for their strong support and encouragement. The remarkable achievements of the HERA machine group were essential for the successful completion of this work and are greatly appreciated. We are grateful for the support of the DESY computing and network services. The design, construction and installation of the ZEUS detector have been made possible owing to the ingenuity and effort of many people from DESY and home institutes who are not listed as authors. The NLO calculations for $W^{\pm}$ production were provided by K.P. Diener, C. Schwanenberger and M. Spira. We would like to thank B. Koblitz for providing his range-searching algorithm, which was used for the calculation of the tau discriminant.

References

[1] H1 Coll., C. Adloff et al., Eur. Phys. J. **C 5**, 575 (1998).

[2] H1 Coll., V. Andreev et al., Phys. Lett. **B 561**, 241 (2003).

[3] ZEUS Coll., J. Breitweg et al., Phys. Lett. **B 471**, 411 (2000).

[4] ZEUS Coll., S. Chekanov et al., Phys. Lett. **B 559**, 153 (2003).

[5] T. Han, R.D. Peccei and X. Zhang, Nucl. Phys. **B 454**, 527 (1995);
V.F. Obraztsov, S.R. Slabospitsky and O.P. Yushchenko, Phys. Lett. **B 426**, 393 (1998);
T. Han et al., Phys. Rev. **B 426**, 073008 (1998);
T. Han and J.L. Hewett, Phys. Rev. **D 60**, 074015 (1999);
H. Fritzsch and D. Holtmannspotter, Phys. Lett. **B 457**, 186 (1999).

[6] J. Butterworth and H. Dreiner, Nucl. Phys. **B 397**, 3 (1993);
T. Kon and T. Kobayashi, Phys. Lett. **B 270**, 81 (1991);
W. Porod, Phys. Rev. **D 59**, 095009 (1999).

[7] ZEUS Coll., U. Holm (ed.), *The ZEUS Detector*. Status Report (unpublished), DESY (1993), available on `http://www-zeus.desy.de/bluebook/bluebook.html`.

[8] ZEUS Coll., M. Derrick et al., Phys. Lett. **B 293**, 465 (1992).

[9] N. Harnew et al., Nucl. Inst. Meth. **A 279**, 290 (1989);
B. Foster et al., Nucl. Phys. Proc. Suppl. **B 32**, 181 (1993);
B. Foster et al., Nucl. Inst. Meth. **A 338**, 254 (1994).

[10] M. Derrick et al., Nucl. Inst. Meth. **A 309**, 77 (1991);
A. Andresen et al., Nucl. Inst. Meth. **A 309**, 101 (1991);
A. Caldwell et al., Nucl. Inst. Meth. **A 321**, 356 (1992);
A. Bernstein et al., Nucl. Inst. Meth. **A 336**, 23 (1993).

[11] J. Andruszków et al., Preprint DESY-92-066, DESY, 1992;
ZEUS Coll., M. Derrick et al., Z. Phys. **C 63**, 391 (1994);
J. Andruszków et al., Acta Phys. Pol. **B 32**, 2025 (2001).

[12] W.H. Smith, K. Tokushuku and L.W. Wiggers. *Proc. Computing in High-Energy Physics (CHEP), Annecy, France, 1992*, C. Verkerk and W. Wojcik (eds.), p.222. CERN, Geneva, Switzerland (1992). Also in preprint DESY-92-150B.

[13] R. Brun et al., GEANT3, Technical Report CERN-DD/EE/84-1, CERN, 1987.

[14] U. Baur, J.A.M. Vermaseren and D. Zeppenfeld, Nucl. Phys. **B 375**, 3 (1992).

[15] T. Sjöstrand, Comp. Phys. Comm. **39**, 347 (1986);
T. Sjöstrand and M. Bengtsson, Comp. Phys. Comm. **43**, 367 (1987);
T. Sjöstrand, Comp. Phys. Comm. **82**, 74 (1994).

[16] S. Jadach, Z. Was and J.H. Kuehn, Comp. Phys. Comm. **64**, 275 (1991).

[17] P. Nason, R. Rückl and M. Spira, J. Phys. **G 25**, 1434 (1999);
M. Spira, Preprint DESY-99-060 (hep-ph/9905469), 1999;
K.P. Diener, C. Schwanenberger and M. Spira, Eur. Phys. J. **C 25**, 405 (2002);
K.P. Diener, C. Schwanenberger and M. Spira, Preprint hep-ex/0302040, 2003.

[18] H.L. Lai et al., Phys. Rev. **D 55**, 1280 (1997).

[19] P. Aurenche et al., Z. Phys. **C 56**, 589 (1992).

[20] K. Charchula, G.A. Schuler and H. Spiesberger, Comp. Phys. Comm. **81**, 381 (1994).

[21] A. Kwiatkowski, H. Spiesberger and H.-J. Möhring, Comp. Phys. Comm. **69**, 155 (1992).

[22] G. Ingelman, A. Edin and J. Rathsman, Comp. Phys. Comm. **101**, 108 (1997).

[23] L. Lönnblad, Comp. Phys. Comm. **71**, 15 (1992).

[24] CTEQ Coll., H.L. Lai et al., Eur. Phys. J. **C 12**, 375 (2000).

[25] M. Bengtsson and T. Sjöstrand, Comp. Phys. Comm. **46**, 43 (1987).

[26] T. Abe, Comp. Phys. Comm. **136**, 126 (2001).

[27] H.J. Kim and S. Kartik, Preprint LSUHE-145-1993, 1993.

[28] C.N. Nguyen. Diploma Thesis, Univ. Hamburg, Hamburg (Germany), Report DESY-THESIS-2002-024, 2002.

[29] S. Catani et al., Nucl. Phys. **B 406**, 187 (1993).

[30] S.D. Ellis and D.E. Soper, Phys. Rev. **D 48**, 3160 (1993).

[31] J.E. Huth et al., *Research Directions for the Decade. Proceedings of Summer Study on High Energy Physics, 1990*, E.L. Berger (ed.), p. 134. World Scientific (1992). Also in preprint FERMILAB-CONF-90-249-E.

[32] ZEUS Coll., S. Chekanov et al., Phys. Lett. **B 531**, 9 (2002).

[33] H1 Coll., C. Adloff et al., Nucl. Phys. **B 545**, 3 (1999).

[34] ZEUS Coll., S. Chekanov et al., Phys. Lett. **B 558**, 41 (2003).

[35] J.R. Forshaw and M.H. Seymour, JHEP **9909**, 009 (1999).

[36] M.H. Seymour, Nucl. Phys. **B 421**, 545 (1994).

[37] D. Dannheim. PhD Thesis, Univ. Hamburg, Hamburg (Germany), Report DESY-THESIS-2003-025, 2003.

[38] ZEUS Coll., S. Chekanov et al., Phys. Rev. **D 65**, 092004 (2002).

[39] T. Carli and B. Koblitz, *Proceedings of the VII International Workshop on Advanced Computing and Analysis Techniques in Physics Research*, P. Bhat and M. Kasemann (eds.), p. 110. American Institute of Physics (2000). Also in hep-ph/0011224;
T. Carli and B. Koblitz, Nucl. Inst. Meth. **A 501**, 576 (2003).

[40] M. Moritz. Ph.D. Thesis, Univ. Hamburg, Hamburg (Germany), Report DESY-THESIS-2002-009, 2002.

[41] ZEUS Coll., J. Breitweg et al., Eur. Phys. J. **C 11**, 427 (1999).

[42] ZEUS Coll., J. Breitweg et al., Z. Phys. **C 74**, 207 (1997).

Selection stage	Obs.	SM exp. ($W^{\pm}$ contrib.)	$\epsilon_{\mathrm{s.top}} \cdot BR$ (%)
Isolated tracks	7	$2.18^{+0.39}_{-0.58}$ (18%)	0.68
Discriminant $\mathcal{D} > 0.95$	3	$0.40^{+0.12}_{-0.13}$ (43%)	0.27
$p_T^{\mathrm{had}} > 25\,\mathrm{GeV}$ (final sel.)	2	$0.20^{+0.05}_{-0.05}$ (49%)	0.27
$p_T^{\mathrm{had}} > 40\,\mathrm{GeV}$	1	$0.07^{+0.02}_{-0.02}$ (71%)	0.25

Table 1: *Event yields for the data from 1994-2000, corresponding background expectations and efficiency times branching ratio for the single-top MC at different selection stages in the search for isolated tau leptons. The percentage of single-W production included in the expectation is indicated in parentheses. The statistical and systematic uncertainties in quadrature are also indicated.*

Quantity	Event 1	Event 2
Missing transverse momentum p_T^{CAL}	37 GeV	39 GeV
Hadronic transverse momentum p_T^{had}	48 GeV	38 GeV
Transverse momentum of the tau-candidate jet p_T^{jet}	21 GeV	41 GeV
Transverse momentum of the tau-candidate track p_T^{trk}	9 GeV	27 GeV
Charge sign of the tau-candidate track	$-$	$+$
Significance in numbers of standard deviations	5.7σ	3.8σ
Acoplanarity of the tau-candidate track $\phi_{\mathrm{acopl}}^{\mathrm{trk}}$	45°	55°
Transverse mass M_T	32 GeV	70 GeV
Discriminant $\mathcal{D}$	0.994	0.977

Table 2: *Selected event variables for the two tau-candidate events at high p_T^{had}.*

ZEUS 1994-2000 $e^{\pm}p$ $\mathcal{L} = 130.1\,\mathrm{pb}^{-1}$	Electron obs./exp. ($W^{\pm}$ contribution)	Muon obs./exp. ($W^{\pm}$ contribution)	Tau obs./exp. ($W^{\pm}$ contribution)
$p_T^{\mathrm{had}} > 25\,\mathrm{GeV}$	2 / 2.90 $^{+0.59}_{-0.32}$ (45%)	5 / 2.75 $^{+0.21}_{-0.21}$ (50%)	2 / 0.20 $^{+0.05}_{-0.05}$ (49%)
$p_T^{\mathrm{had}} > 40\,\mathrm{GeV}$	0 / 0.94 $^{+0.11}_{-0.10}$ (61%)	0 / 0.95 $^{+0.14}_{-0.10}$ (61%)	1 / 0.07 $^{+0.02}_{-0.02}$ (71%)

Table 3: *Summary of the results of searches for events with isolated leptons, missing transverse momentum and large p_T^{had}. The number of observed events is compared to the SM prediction. The $W^{\pm}$ component is given in parentheses in percent. The statistical and systematic uncertainties added in quadrature are also indicated. The results for the electron and the muon channel were obtained from a previous search [4].*

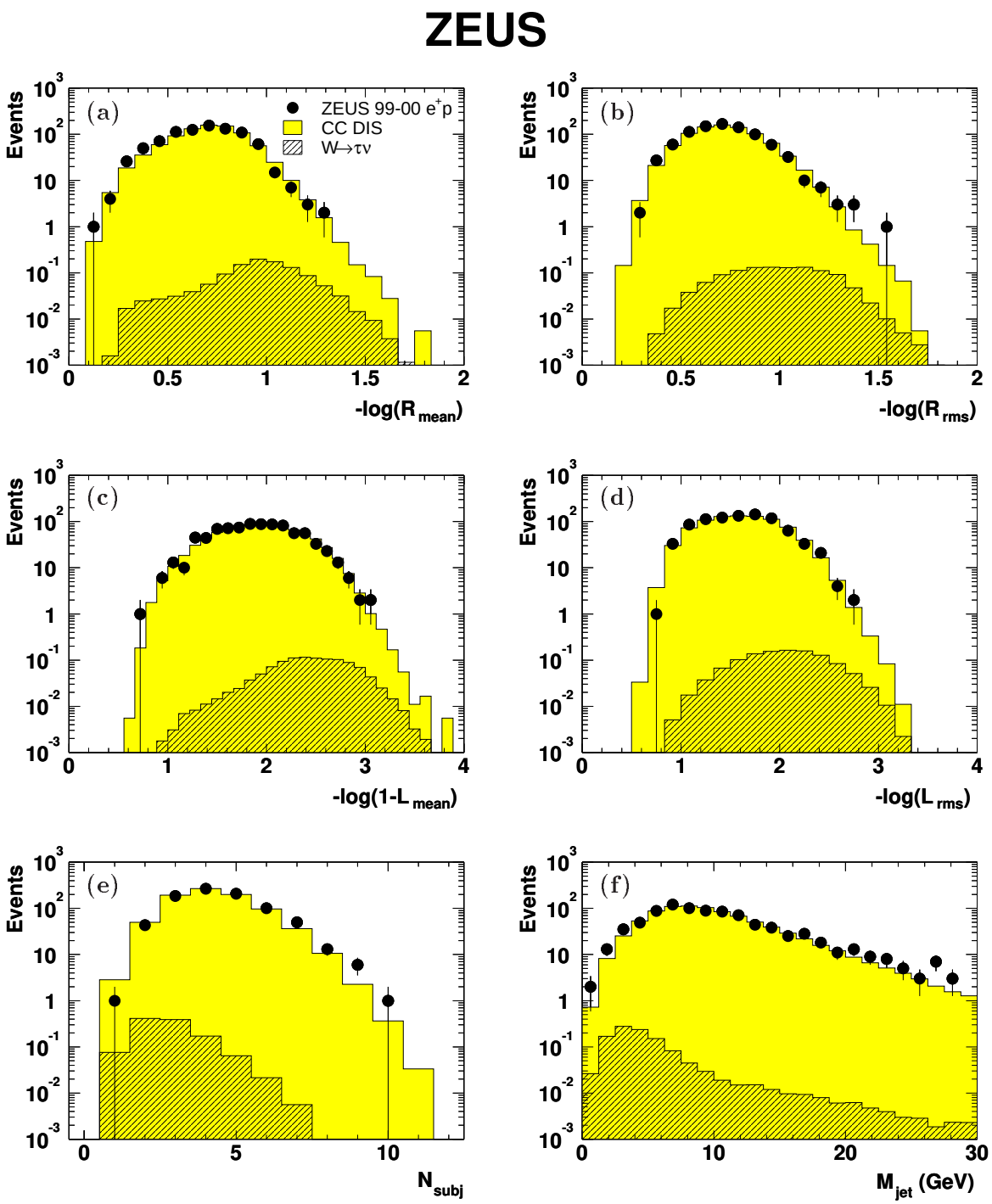

Figure 1: *Observables characterising the internal jet structure for an inclusive selection of CC DIS events (see text for definitions). Shown are the data (dots), the simulation of CC DIS events (shaded histograms) and the simulation of the direct $W^{\pm}$-production signal $W^{\pm} \to \overset{(-)}{\nu}_{\tau}\tau^{\pm}$, where the τ decays hadronically (hatched histograms).*

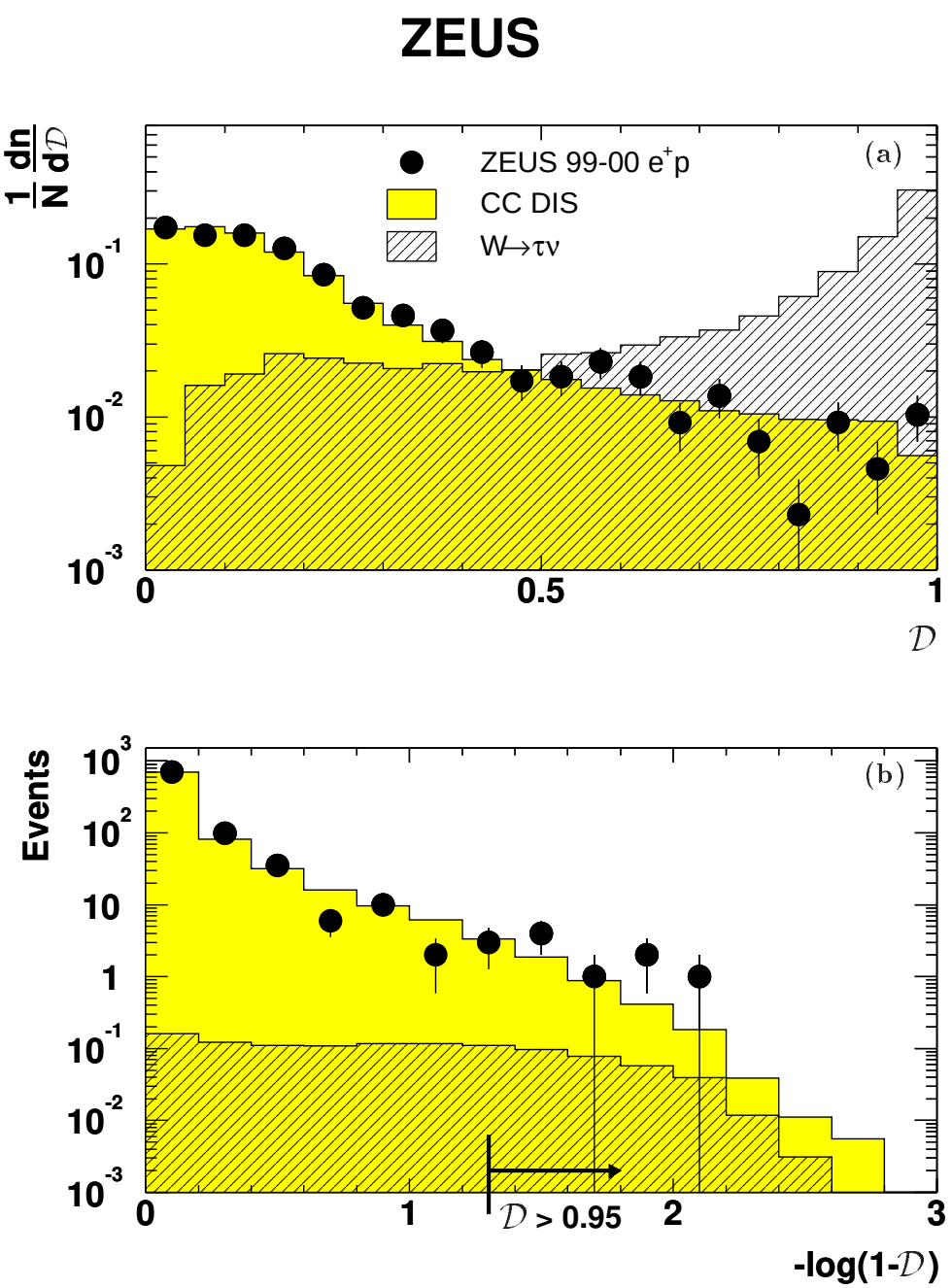

Figure 2: *Distribution of the tau discriminant, $\mathcal{D}$, for an inclusive selection of CC DIS data events (dots), a simulation of CC DIS events (shaded histograms) and the simulation of the direct $W^{\pm}$-production signal $W^{\pm} \to \overset{(-)}{\nu}_{\tau}\tau^{\pm}$, where the τ decays hadronically (hatched histograms). In each event, only the jet with the highest value of the discriminant enters. The histograms are normalised (a) to the total number of events N and (b) to the luminosity of the data. In (b), the $-\log(1-\mathcal{D})$ distribution is displayed to expand the region in which the tau lepton signal is expected.*

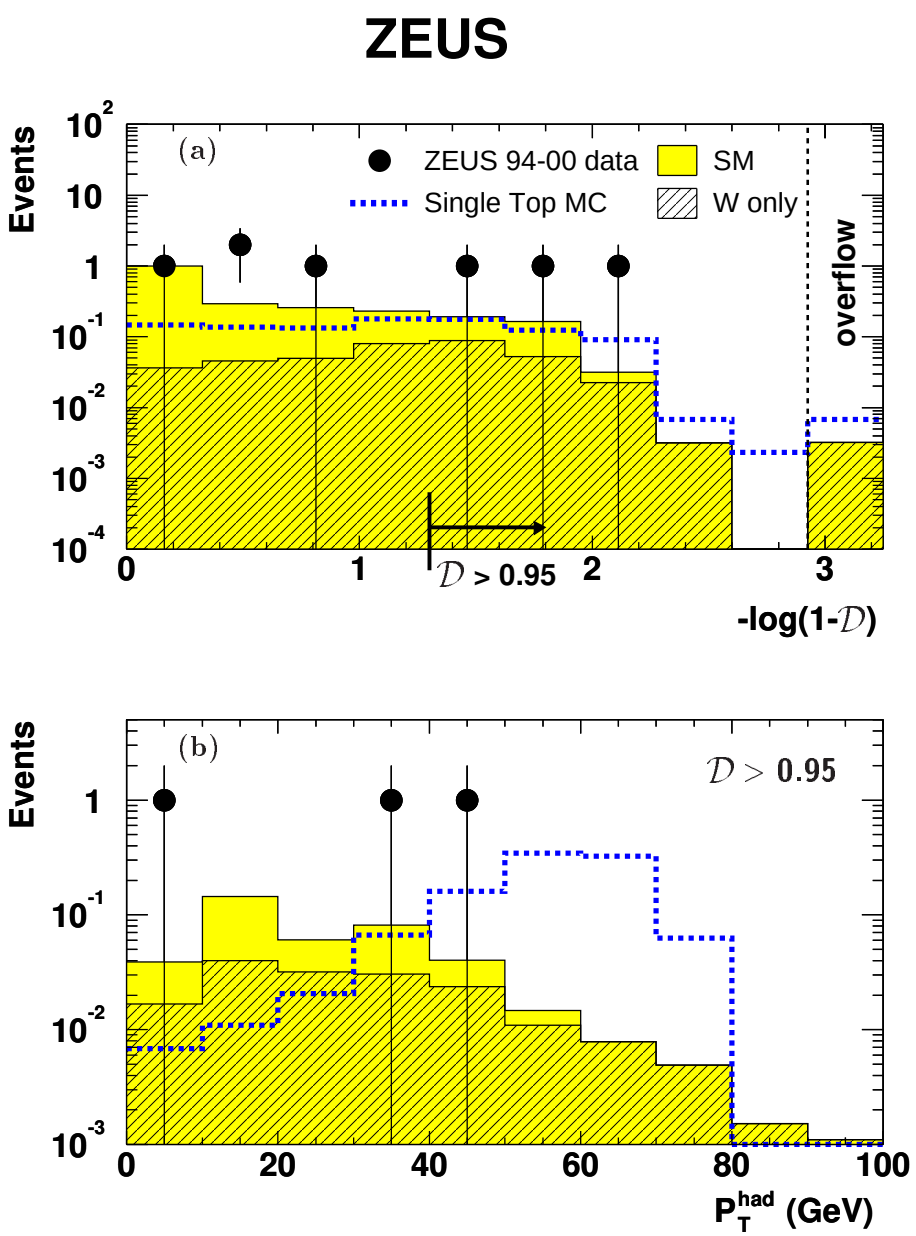

Figure 3: *Distribution of (a) the tau discriminant, $-\log(1-\mathcal{D})$, for the tau preselection before applying the cut $\mathcal{D} > 0.95$ and (b) the hadronic transverse momentum, $p_T^{\rm had}$, after applying the cut $\mathcal{D} > 0.95$. The data (points) are compared to the SM expectations (shaded histogram). The hatched histogram represents the contribution from $W^{\pm}$ boson production in the SM. The dashed line represents the distribution of the single-top MC, including all decay channels of the $W^{\pm}$ boson, normalised to an integral of one event.*

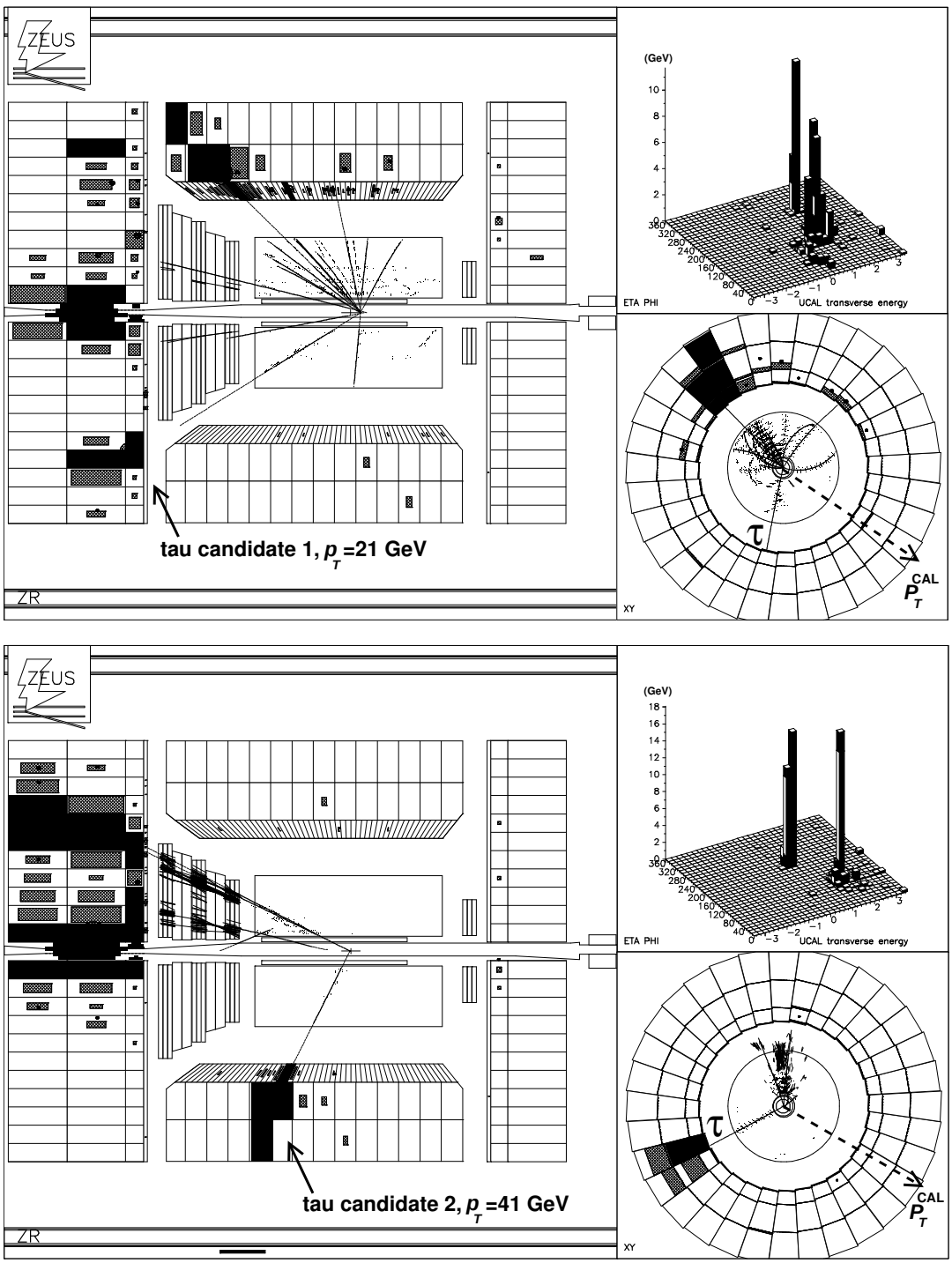

Figure 4: *Tau-candidate events from e^+p interactions at $\sqrt{s} = 318\,GeV$ in the ZEUS detector. The energy deposition in the CAL is proportional to the size and density of shading in the CAL cells. The lego plot shows the CAL energy deposition projected in the $\{\eta, \phi\}$-plane. In the x-y-view, only the energy deposition in the barrel calorimeter is shown. The dashed arrow in the x-y view indicates the direction of the missing transverse momentum in the calorimeter, $p_T^{\rm CAL}$. Selected event variables for the two candidates are given in Table 2.*